

See discussions, stats, and author profiles for this publication at: <https://www.researchgate.net/publication/221738232>

Low values of 5-hydroxymethylcytosine (5hmC), the “sixth base,” are associated with anaplasia in human brain tumors

ARTICLE *in* INTERNATIONAL JOURNAL OF CANCER · OCTOBER 2012

Impact Factor: 5.09 · DOI: 10.1002/ijc.27429 · Source: PubMed

CITATIONS

56

READS

29

13 AUTHORS, INCLUDING:



Theo F. J. Kraus

Ludwig-Maximilians-University of Munich

14 PUBLICATIONS 183 CITATIONS

SEE PROFILE



Daniel Globisch

Uppsala University

28 PUBLICATIONS 793 CITATIONS

SEE PROFILE



Martin Münzel

University of Oxford

21 PUBLICATIONS 1,184 CITATIONS

SEE PROFILE



Ulrich Schüller

Ludwig-Maximilians-University of Munich

85 PUBLICATIONS 2,034 CITATIONS

SEE PROFILE

Low values of 5-hydroxymethylcytosine (5hmC), the “sixth base,” are associated with anaplasia in human brain tumors

Theo F.J. Kraus^{1*}, Daniel Globisch^{2*}, Mirko Wagner², Sabina Eigenbrod¹, David Widmann¹, Martin Münzel², Markus Müller², Toni Pfaffeneder², Benjamin Hackner², Wolfgang Feiden³, Ulrich Schüller¹, Thomas Carell² and Hans A. Kretzschmar¹

¹ Center for Neuropathology and Prion Research (ZNP), Ludwig-Maximilians-University, Munich, Germany

² Department of Chemistry, Center for Integrated Protein Science (CIPS^M), Ludwig-Maximilians-University, Munich, Germany

³ Institute for Neuropathology, University Hospital Homburg, Homburg, Germany

5-Methylcytosine (5mC) in genomic DNA has important epigenetic functions in embryonic development and tumor biology. 5-Hydroxymethylcytosine (5hmC) is generated from 5mC by the action of the TET (Ten-Eleven-Translocation) enzymes and may be an intermediate to further oxidation and finally demethylation of 5mC. We have used immunohistochemistry (IHC) and isotope-based liquid chromatography mass spectrometry (LC-MS) to investigate the presence and distribution of 5hmC in human brain and brain tumors. In the normal adult brain, IHC identified 61.5% 5hmC positive cells in the cortex and 32.4% 5hmC in white matter (WM) areas. In tumors, positive staining of cells ranged from 1.1% in glioblastomas (GBMs) (WHO Grade IV) to 8.9% in Grade I gliomas (pilocytic astrocytomas). In the normal adult human brain, LC-MS also showed highest values in cortical areas (1.17% 5hmC/dG [deoxyguanosine]), in the cerebral WM we measured around 0.70% 5hmC/dG. 5hmC levels were related to tumor differentiation, ranging from lowest values of 0.078% 5hmC/dG in GBMs (WHO Grade IV) to 0.24% 5hmC/dG in WHO Grade II diffuse astrocytomas. 5hmC measurements were unrelated to 5mC values. We find that the number of 5hmC positive cells and the amount of 5hmC/dG in the genome that has been proposed to be related to pluripotency and lineage commitment in embryonic stem cells is also associated with brain tumor differentiation and anaplasia.

Epigenetics, the study of mechanisms that control gene expression (in a potentially heritable way), may be the most rapidly expanding field in tumor biology. On a molecular level, (i) DNA methylation, *i.e.*, covalent modification of cytosine bases resulting in 5-methylcytosine (5mC), (ii) histone modifications and (iii) nucleosome positioning are regarded as the driving epigenetic mechanisms. They are fundamental to the regulation of many cellular processes, including gene and micro

RNA expression, DNA-protein interactions, suppression of transposable element mobility, cellular differentiation, embryogenesis, X-chromosome inactivation and genomic imprinting.

In tumor biology, DNA methylation is the best-studied epigenetic change. Epigenetic silencing of O⁶-methylguanine DNA-methyltransferase (MGMT)¹ has been described as a strong predictive factor of treatment response to chemotherapy with alkylating agents of glioblastoma (GBM) and anaplastic astrocytoma (AA).² Methylation of CpG islands in the MGMT promoter with ensuing repression of MGMT transcriptional activity is generally viewed as the cause for this correlation.³

Oxidation of 5mC leading to 5-hydroxymethylcytosine (5hmC) has been identified as a new epigenetic phenomenon in mouse Purkinje cells.⁴ Three possible modes of action of 5hmC were discussed. (i) It might influence chromatin structure and local transcriptional activity by recruiting selective 5hmC-binding proteins or excluding 5mC-binding proteins. (ii) Conversion of 5mC to 5hmC might facilitate passive DNA demethylation by excluding the maintenance DNMT1, which recognizes 5hmC poorly. (iii) 5hmC may be an intermediate in a pathway of active DNA demethylation either by conversion to cytosine under certain conditions or by replacement of 5hmC by specific DNA repair mechanisms. Most recent findings support the hypothesis that 5hmC is an intermediate in a pathway for active DNA demethylation.^{5–7} The TET proteins, identified as a new family of enzymes that

Key words: epigenetics, brain tumors, 5-hydroxymethylcytosine, 5hmC, glioma, ependymoma, meningioma, IDH, TET

Grant sponsor: DFG Normalverfahren; **Grant numbers:** CA275/8-4, SFB 749, SFB 646; **Grant sponsor:** Fonds der Chemischen Industrie

DOI: 10.1002/ijc.27429

History: Received 18 Oct 2011; Accepted 29 Dec 2011; Online 10 Jan 2012

*T.F.J.K. and D.G. contributed equally to this work.

Correspondence to: Hans A. Kretzschmar, Center for Neuropathology and Prion Research (ZNP), Ludwig-Maximilians-University, 81377 Munich, Germany, E-mail: hans.kretzschmar@med.uni-muenchen.de or Thomas Carell, Center for Integrated Protein Science (CIPS^M), Department of Chemistry, Ludwig-Maximilians-University, 81377 Munich, Germany, E-mail: thomas.carell@cup.uni-muenchen.de

Table 1. Twenty-two tissue samples were selected from nine control cases from the BrainBank Munich

Case	Sample	Age	Gender	Postmortem time (h)	Region	Cause of death	5hmC positive cells (%)	5mC/dG (%)	5hmC/dG (%)
1	a	85	F	20	Occipital cortex	Cardiac arrest	55.05	5.16	1.17
1	b	85	F	20	Occipital white matter	Cardiac arrest	19.07	4.26	0.76
1	c	85	F	20	Frontal cortex	Cardiac arrest	70.29	–	–
1	d	85	F	20	Frontal white matter	Cardiac arrest	23.27	–	–
2	a	61	M	24	Frontal cortex	Cardiac arrest	55.46	5.05	1.06
2	b	61	M	24	Frontal white matter	Cardiac arrest	16.45	–	–
3	a	87	M	48	Frontal cortex	Cardiac arrest	54.32	5.94	1.13
3	b	87	M	48	Frontal white matter	Cardiac arrest	22.85	–	–
3	c	87	M	48	Occipital cortex	Cardiac arrest	54.70	5.64	1.14
3	d	87	M	48	Occipital white matter	Cardiac arrest	23.08	4.23	0.64
4	a	46	M	n.a.	Occipital cortex	Cardiac arrest	64.29	5.74	1.12
4	b	46	M	n.a.	Occipital white matter	Cardiac arrest	36.34	4.36	0.54
5	a	84	M	19	Frontal white matter	Cardiac arrest	28.57	3.82	0.78
5	b	84	M	19	Frontal cortex	Cardiac arrest	59.92	4.55	1.19
6	a	61	M	n.a.	Frontal white matter	Cardiac arrest	61.61	4.14	0.76
6	b	61	M	n.a.	Frontal cortex	Cardiac arrest	70.33	5.35	1.35
7	a	26	F	n.a.	Frontal cortex	Hemorrhagic pericard effusion	80.17	–	–
7	b	26	F	n.a.	Frontal white matter	Hemorrhagic pericard effusion	58.06	–	–
8	a	41	M	n.a.	Frontal cortex	Multiple organ failure	65.02	–	–
8	b	41	M	n.a.	Frontal white matter	Multiple organ failure	38.70	–	–
9	a	39	M	n.a.	Frontal cortex	Haematothorax	46.75	–	–
9	b	39	M	n.a.	Frontal white matter	Haematothorax	30.00	–	–

alter the methylation status of DNA, are 2-oxoglutarate (2OG)- and Fe(II)-dependent enzymes that catalyze the conversion of 5mC to 5hmC,⁸ 5-formylcytosine and 5-carboxylcytosine.^{5–7} TET proteins and 5hmC have been reported in various tissues and both are tightly regulated during embryonic stem cells (ESC) differentiation.⁹ 5hmC content has been described as significantly reduced in stem cell/progenitor cell compartments and in human cancers (prostate, breast and colon).¹⁰

To obtain a first insight into a possible role of 5hmC in the human brain, we used isotope-based liquid chromatography mass spectrometry (LC-MS) to measure 5hmC concentrations in various cortical and white matter regions of the adult human brain to elucidate whether hydroxymethylation may be present in human brain tumors, we measured 5hmC content in slowly growing frequent brain tumors, *i.e.*, astrocytomas WHO Grades I, II and rapidly growing AAs WHO Grade III and GBMs (WHO Grade IV)¹¹ and other brain tumors. In addition, we used immunohistochemistry (IHC) to investigate the distribution of 5hmC in the brain and in brain tumor cells.

Material and Methods

Sample selection normal brain regions

To evaluate the amount of 5hmC in human brain, we selected tissue of nine donors that had provided their brains

for research purposes after death. The samples were obtained from the Brain Bank Munich. As target regions we selected frontal cortex, occipital cortex, frontal white matter and occipital white matter. The tissue samples had either been formalin-fixed and paraffin-embedded (FFPE) or stored at -80°C . For this study, we chose 22 human control samples, well characterized by age and gender (Table 1). The age of the patients varied from 26 to 87 with a mean age of 59 years.

Sample selection tumors

To evaluate 5hmC in human brain tumors, we used FFPE and frozen material that had been stored at -80°C . The samples were obtained from the Brain Tumor Bank, Center for Neuropathology, LMU Munich, as well as from the Brain Tumor Bank of the Institute for Neuropathology, University Hospital Homburg. For this study, we selected areas consisting of more than 75% of tumor cells as estimated from freshly made and H&E stained sections. In each case we separated clearly visible tumor areas. One hundred seventeen human tumor samples derived from 117 different tumors were selected, including 80 astrocytomas and GBMs, 23 ependymomas and 14 meningiomas (Table 2). The age of the patients ranged from 3 to 81 years with a mean of 46 years and the male to female ratio was 67:43. In the astrocytoma

Table 2. One hundred seventeen tumor samples were selected from the Brain Tumour Bank, Center for Neuropathology, LMU Munich and the Brain Tumour Bank of the Institute for Neuropathology, University Hospital Homburg

Case	Age	Gender	Tumor	Grade	Region	5hmC positive cells (%)	5mC/dG (%)	5hmC/dG (%)	IDH status
1	15	M	Pilocytic astrocytoma (WHO Grade I)	I	Temporal	13.66	4.75	0.18	No mutation
2	23	F	Pilocytic astrocytoma (WHO Grade I)	I	Thoracic spine	10.83	4.10	0.24	No mutation
3	23	M	Pilocytic astrocytoma (WHO Grade I)	I	n.a.	7.69	4.58	0.24	No mutation
4	12	F	Pilocytic astrocytoma (WHO Grade I)	I	Rhombencephalon	10.03	4.99	0.17	No mutation
5	9	M	Pilocytic astrocytoma (WHO Grade I)	I	Cerebellum	1.66	4.98	0.12	No mutation
6	21	M	Pilocytic astrocytoma (WHO Grade I)	I	Temporal	9.57	–	–	No mutation
7	34	M	Diffuse astrocytoma (WHO Grade II)	II	Fronto-temporal	3.75	4.66	0.17	Mutation
8	35	M	Diffuse astrocytoma (WHO Grade II)	II	Insula	1.47	–	–	Mutation
9	36	F	Diffuse astrocytoma (WHO Grade II)	II	Occipital	0.72	–	–	Mutation
10	15	M	Diffuse astrocytoma (WHO Grade II)	II	Thalamus	3.35	–	–	No mutation
11	28	F	Diffuse astrocytoma (WHO Grade II)	II	Precentral	1.55	–	–	Mutation
12	n.a.	n.a.	Diffuse astrocytoma (WHO Grade II)	II	n.a.	–	4.50	0.09	Mutation
13	n.a.	n.a.	Diffuse astrocytoma (WHO Grade II)	II	n.a.	–	4.57	0.24	Mutation
14	44	M	Diffuse astrocytoma (WHO Grade II)	II	Insula	7.04	–	–	No mutation
15	66	F	Diffuse astrocytoma (WHO Grade II)	II	Insula	5.19	–	–	No mutation
16	35	M	Diffuse astrocytoma (WHO Grade II)	II	Pons	9.06	–	–	No mutation
17	41	F	Diffuse astrocytoma (WHO Grade II)	II	Tectum	11.89	–	–	No mutation
18	30	M	Diffuse astrocytoma (WHO Grade II)	II	Temporal	0.00	–	–	Mutation
19	3	M	Diffuse astrocytoma (WHO Grade II)	II	Basal Ganglia	–	5.53	0.46	No mutation
20	74	M	Anaplastic astrocytoma (WHO Grade III)	III	Fronto-temporal	0.59	4.40	0.08	Mutation
21	43	M	Anaplastic astrocytoma (WHO Grade III)	III	Frontal	–	4.34	0.08	Mutation
22	41	F	Anaplastic astrocytoma (WHO Grade III)	III	Parietal	–	4.51	0.10	Mutation
23	59	M	Anaplastic astrocytoma (WHO Grade III)	III	n.a.	7.27	–	–	No mutation
24	62	M	Anaplastic astrocytoma (WHO Grade III)	III	Central	3.72	–	–	Mutation
25	41	M	Anaplastic astrocytoma (WHO Grade III)	III	Frontal	2.40	–	–	Mutation
26	37	F	Anaplastic astrocytoma (WHO Grade III)	III	Frontal	2.29	–	–	Mutation
27	37	F	Anaplastic astrocytoma (WHO Grade III)	III	Temporal	2.68	–	–	No mutation
28	31	M	Anaplastic astrocytoma (WHO Grade III)	III	Temporal	0.80	–	–	Mutation
29	32	M	Anaplastic astrocytoma (WHO Grade III)	III	Temporal	2.69	–	–	Mutation
30	42	M	Anaplastic astrocytoma (WHO Grade III)	III	Temporal	0.13	–	–	Mutation
31	44	F	Anaplastic astrocytoma (WHO Grade III)	III	n.a.	6.85	–	–	No mutation
32	44	F	Anaplastic astrocytoma (WHO Grade III)	III	Frontal	4.86	–	–	No mutation
33	81	F	Anaplastic astrocytoma (WHO Grade III)	III	Cerebellum	1.11	–	–	No mutation
34	70	M	Anaplastic astrocytoma (WHO Grade III)	III	Temporal	5.35	–	–	No mutation
35	61	M	Anaplastic astrocytoma (WHO Grade III)	III	Thalamus	6.00	–	–	No mutation
36	53	M	Anaplastic astrocytoma (WHO Grade III)	III	Temporo-mesial	–	4.76	0.30	No mutation
37	50	M	Anaplastic astrocytoma (WHO Grade III)	III	Temporal	–	3.79	0.10	No mutation
38	72	M	Glioblastoma multiforme (WHO Grade IV)	IV	Temporoparietal	0.37	4.35	0.16	No mutation
39	47	M	Glioblastoma multiforme (WHO Grade IV)	IV	Frontal	–	4.33	0.13	No mutation
40	61	M	Glioblastoma multiforme (WHO Grade IV)	IV	Parietal	2.26	4.06	0.10	No mutation
41	69	F	Glioblastoma multiforme (WHO Grade IV)	IV	Occipital	0.25	3.77	0.09	No mutation

Table 2. One hundred seventeen tumor samples were selected from the Brain Tumour Bank, Center for Neuropathology, LMU Munich and the Brain Tumour Bank of the Institute for Neuropathology, University Hospital Homburg (Continued)

Case	Age	Gender	Tumor	Grade	Region	5hmC positive cells (%)	5mC/dG (%)	5hmC/dG (%)	IDH status
42	55	M	Glioblastoma multiforme (WHO Grade IV)	IV	Parietal	0.08	5.58	0.03	No mutation
43	44	F	Glioblastoma multiforme (WHO Grade IV)	IV	Frontal	0.28	4.70	0.09	No mutation
44	64	M	Glioblastoma multiforme (WHO Grade IV)	IV	Parietal	0.97	4.32	0.07	No mutation
45	25	F	Glioblastoma multiforme (WHO Grade IV)	IV	Frontal	1.37	4.70	0.03	Mutation
46	66	M	Glioblastoma multiforme (WHO Grade IV)	IV	Temporal	3.48	4.27	0.05	No mutation
47	64	M	Glioblastoma multiforme (WHO Grade IV)	IV	Temporal	0.49	4.06	0.11	No mutation
48	67	F	Glioblastoma multiforme (WHO Grade IV)	IV	Temporal	0.00	–	–	No mutation
49	67	M	Glioblastoma multiforme (WHO Grade IV)	IV	Occipital	0.55	–	–	No mutation
50	41	M	Glioblastoma multiforme (WHO Grade IV)	IV	Temporal	0.67	–	–	No mutation
51	66	M	Glioblastoma multiforme (WHO Grade IV)	IV	Temporal	1.82	–	–	No mutation
52	58	M	Glioblastoma multiforme (WHO Grade IV)	IV	Parietal	1.82	–	–	No mutation
53	30	M	Glioblastoma multiforme (WHO Grade IV)	IV	Temporal	1.22	–	–	Mutation
54	69	F	Glioblastoma multiforme (WHO Grade IV)	IV	Temporal	1.45	–	–	No mutation
55	53	f	Glioblastoma multiforme (WHO Grade IV)	IV	Frontal	1.60	–	–	No mutation
56	43	M	Glioblastoma multiforme (WHO Grade IV)	IV	Temporo-parieto-occipital	2.21	–	–	No mutation
57	59	M	Glioblastoma multiforme (WHO Grade IV)	IV	Temporal	1.14	–	–	No mutation
58	7	M	Glioblastoma multiforme (WHO Grade IV)	IV	Thalamus	2.28	–	–	No mutation
59	67	M	Glioblastoma multiforme (WHO Grade IV)	IV	Temporal	0.78	–	–	No mutation
60	64	F	Glioblastoma multiforme (WHO Grade IV)	IV	Temporo-mesial	1.61	–	–	No mutation
61	43	F	Glioblastoma multiforme (WHO Grade IV)	IV	Frontal	1.19	–	–	Mutation
62	72	M	Glioblastoma multiforme (WHO Grade IV)	IV	Temporal	1.49	–	–	No mutation
63	32	M	Glioblastoma multiforme (WHO Grade IV)	IV	Temporal	0.53	–	–	Mutation
64	33	M	Glioblastoma multiforme (WHO Grade IV)	IV	Temporal	1.20	–	–	Mutation
65	46	M	Glioblastoma multiforme (WHO Grade IV)	IV	Temporal	1.92	–	–	Mutation
66	40	F	Glioblastoma multiforme (WHO Grade IV)	IV	Parieto-occipital	0.96	–	–	Mutation
67	38	M	Glioblastoma multiforme (WHO Grade IV)	IV	Temporal	0.60	–	–	Mutation
68	61	M	Glioblastoma multiforme (WHO Grade IV)	IV	Temporal	0.31	–	–	No mutation
69	47	M	Glioblastoma multiforme (WHO Grade IV)	IV	Temporal	0.62	–	–	No mutation
70	78	M	Glioblastoma multiforme (WHO Grade IV)	IV	Temporal	0.38	–	–	No mutation
71	71	F	Glioblastoma multiforme (WHO Grade IV)	IV	Frontal	1.23	–	–	No mutation
72	62	F	Glioblastoma multiforme (WHO Grade IV)	IV	Temporal	0.43	–	–	No mutation
73	64	F	Glioblastoma multiforme (WHO Grade IV)	IV	Frontal	1.89	–	–	No mutation
74	70	M	Glioblastoma multiforme (WHO Grade IV)	IV	Parietal	0.87	–	–	No mutation
75	41	F	Glioblastoma multiforme (WHO Grade IV)	IV	Parietal	0.40	–	–	No mutation
76	74	M	Glioblastoma multiforme (WHO Grade IV)	IV	Postcentral	0.53	–	–	No mutation
77	55	M	Glioblastoma multiforme (WHO Grade IV)	IV	Thalamus	0.60	–	–	No mutation
78	37	F	Glioblastoma multiforme (WHO Grade IV)	IV	Frontal	–	4.36	0.08	Mutation
79	34	M	Glioblastoma multiforme (WHO Grade IV)	IV	Frontal	–	4.03	0.04	Mutation
80	34	F	Glioblastoma multiforme (WHO Grade IV)	IV	Temporal	–	3.68	0.04	Mutation
81	30	F	Myxopapillary ependymoma (WHO Grade I)	I	Lumbal spine	44.14	5.19	0.09	n.a.
82	68	M	Subependymoma (WHO Grade I)	I	Rhombencephalon	36.50	4.57	0.42	n.a.

Table 2. One hundred seventeen tumor samples were selected from the Brain Tumour Bank, Center for Neuropathology, LMU Munich and the Brain Tumour Bank of the Institute for Neuropathology, University Hospital Homburg (Continued)

Case	Age	Gender	Tumor	Grade	Region	5hmC positive cells (%)	5mC/dG (%)	5hmC/dG (%)	IDH status
83	20	M	Subependymoma (WHO Grade I)	I	Lateral ventricle	13.54	–	–	n.a.
84	59	M	Subependymoma (WHO Grade I)	I	Lateral ventricle	28.95	–	–	n.a.
85	54	M	Subependymoma (WHO Grade I)	I	Rhombencephalon	16.49	4.55	0.35	n.a.
86	46	F	Subependymoma (WHO Grade I)	I	Thoracic spine	1.28	–	–	n.a.
87	46	F	Subependymoma (WHO Grade I)	I	Lateral ventricle	16.81	–	–	n.a.
88	46	M	Subependymoma (WHO Grade I)	I	Rhombencephalon	15.22	–	–	n.a.
89	n.a.	n.a.	Subependymoma (WHO Grade I)	I	n.a.	–	4.63	0.20	n.a.
90	n.a.	n.a.	Subependymoma (WHO Grade I)	I	n.a.	–	4.58	0.37	n.a.
91	30	F	Ependymoma (WHO Grade II)	II	Filum	20.09	5.04	0.09	n.a.
92	41	M	Ependymoma (WHO Grade II)	II	Cervical spine	5.15	4.74	0.17	n.a.
93	39	M	Ependymoma (WHO Grade II)	II	Cervical spine	6.26	3.38	0.25	n.a.
94	70	F	Ependymoma (WHO Grade II)	II	Cervical spine	15.85	3.70	0.41	n.a.
95	23	M	Ependymoma (WHO Grade II)	II	Thoracic spine	14.43	6.16	0.21	n.a.
96	54	M	Ependymoma (WHO Grade II)	II	Cervical spine	10.86	5.01	0.12	n.a.
97	42	M	Ependymoma (WHO Grade II)	II	n.a.	12.02	–	–	n.a.
98	76	F	Ependymoma (WHO Grade II)	II	Lumbal spine	15.04	–	–	n.a.
99	21	M	Cellular ependymoma (WHO Grade II)	II	Lateral ventricle	12.49	5.05	0.13	n.a.
100	4	M	Anaplastic ependymoma (WHO Grade III)	III	Rhombencephalon	24.16	4.95	0.23	n.a.
101	5	F	Anaplastic ependymoma (WHO Grade III)	III	Posterior cranial fossa	10.47	4.22	0.03	n.a.
102	59	F	Anaplastic ependymoma (WHO Grade III)	III	Thoracic spine	16.59	4.78	0.32	n.a.
103	6	F	Anaplastic ependymoma (WHO Grade III)	III	Lateral ventricle	1.25	–	–	n.a.
104	72	F	Transitional meningioma (WHO Grade I)	I	Fronto-basal	32.12	4.48	0.12	n.a.
105	22	F	Meningothelomatous meningioma (WHO Grade I)	I	Frontal	29.06	4.04	0.17	n.a.
106	60	F	Transitional meningioma (WHO Grade I)	I	Cerebellum	9.52	4.08	0.20	n.a.
107	59	M	Fibrous meningioma (WHO Grade I)	I	Occipital	6.82	–	–	n.a.
108	28	M	Meningothelial meningioma (WHO Grade I)	I	Precentral	18.30	–	–	n.a.
109	79	F	Meningothelial meningioma (WHO Grade I)	I	Temporal	12.46	–	–	n.a.
110	61	M	Atypical meningioma (WHO Grade II)	II	Frontal	1.11	4.65	0.08	n.a.
111	33	F	Chordoid meningioma (WHO Grade II)	II	Frontal	5.24	–	–	n.a.
112	72	F	Atypical meningioma (WHO Grade II)	II	Frontal	14.34	–	–	n.a.
113	79	F	Atypical meningioma (WHO Grade II)	II	Frontal	2.93	4.44	0.11	n.a.
114	26	M	Atypical meningioma (WHO Grade II)	II	Skullbase	8.94	–	–	n.a.
115	n.a.	n.a.	Atypical meningioma (WHO Grade II)	II	n.a.	–	4.24	0.27	n.a.
116	n.a.	n.a.	Atypical meningioma (WHO Grade II)	II	n.a.	–	4.29	0.08	n.a.
117	n.a.	n.a.	Atypical meningioma (WHO Grade II)	II	n.a.	–	3.98	0.16	n.a.

and GBM group, the mean age was 47 years, in ependymomas 40 years and in meningiomas 54 years.

Immunohistochemistry and cell counting

FFPE tissue samples were used for IHC. Standard protocols were followed, in brief 4-µm FFPE sections were deparaffi-

nized by subsequent incubation in xylene (30 min), 100% ethanol (10 min), 96% ethanol (5 min) and 70% ethanol (5 min). The sections were then treated with 2N HCl (35°C, 20 min), pre-incubated with blocking solution (3% I-Block Protein-Based Blocking Reagent (Applied Biosystems, Darmstadt, Germany)) and incubated with the diluted primary

antibody for 18 hr at 4°C. As primary antibody, we used polyclonal rabbit anti-5hmC diluted 1:1,000 (Active Motif, Rixensart, Belgium). Subsequently, the sections were treated with Super Sensitive Polymer-Horseradish peroxidase (HRP) Detection System (BioGenix, San Ramon, CA), followed by incubation in 3,3'-diaminobenzidine (DAB) for 5 min and staining in hemalum. For immunofluorescence staining, we followed standard protocols. As primary antibody, we used polyclonal rabbit anti-5hmC diluted 1:1,000 (Active Motif, Rixensart, Belgium) and monoclonal mouse anti-Ki-67 diluted 1:500 (Dako, Hamburg, Germany). As secondary antibodies, we used Alexa Fluor 488 goat-anti-rabbit IgG diluted 1:300 (Invitrogen, Darmstadt, Germany) and Alexa Fluor 546 goat-anti-mouse IgG diluted 1:300 (Roth, Karlsruhe, Germany). For nuclear staining, we used 4',6-diamidin-2-phenylindol (Roth, Karlsruhe, Germany). Finally, we used Dako fluorescence mounting medium (Dako, Hamburg, Germany).

For cell counting, randomly selected sections were photographed at $\times 10$ and $\times 20$ magnification depending on tissue type and size. Following that at least 200 cells were counted in each case.

To identify IDH1 mutations in astrocytoma and GBM, FFPE samples were stained using the monoclonal mouse IDH1^{R132H} antibody (Dianova, Hamburg, Germany), diluted 1:20, according to the manufacturer's protocol on a Ventana BenchMark system (Roche, Basel, Switzerland).

DNA extraction

For LC-MS, DNA isolation was performed on the basis of the QIAamp DNA Mini Kit (Qiagen, Hilden, Germany) according to the manufacturer's protocol with slight modifications. The RNA digestion was executed twice and instead of column purification phenol extraction was performed, i.e., after addition of buffer AL, the sample was mixed and incubated. The sample was distributed equally to two 2 mL reaction tubes, if necessary. A 1/1 mixture of Roti®Phenol/chloroform (1 vol) was added and the tube was shaken vigorously at RT for 5 min. The tube was centrifuged (12,100g, 15 min) and the aqueous layer was collected. This procedure was repeated once. To the obtained aqueous layer chloroform (1 vol) was added and the tube was shaken at RT for 1 min. After centrifugation (12,100g, 5 min) the aqueous layer was collected. During collection of the aqueous layer, special care was taken to include the interphase. The sample was distributed equally to two 2 mL reaction tubes, if necessary. Ethanol (3 vol) was added. The sample was left to stand at RT for approximately 2 h. After precipitation of the DNA the tube was centrifuged (12,100g, 30 min). The supernatant was discarded and the pellet was dried. Subsequently, it was dissolved in water (100–400 μ L). The solution was centrifuged (12,100g, 30 min) and the supernatant was collected.

Additionally, we isolated DNA from FFPE samples for IDH mutation analysis using a Maxwell 16 system (Promega, Madison, WI) and Maxwell 16 FEV FFPE kit (Promega, Madison, WI) according to the manufacturer's protocols.

Enzymatic digestion

For the enzymatic digestion DNA mixtures (4–10 μ g in a final volume of 100 μ L H₂O) were heated to 100°C for 5 min to denature the DNA and rapidly cooled on ice. After addition of standard solutions, buffer A (10 μ L, 300 mM ammonium acetate, 100 mM CaCl₂, 1 mM ZnSO₄, pH 5.7) and nuclease S1 (80 units, *Aspergillus oryzae*) the mixture was incubated for 3 hr at 37°C. Addition of buffer B (12 μ L, 500 mM Tris-HCl, 1 mM EDTA), antarctic phosphatase (10 units), snake venom phosphodiesterase I (0.2 units, *Crotalus adamanteus* venom) and incubation for further 3 hr at 37°C completed the digestion. Labeled nucleosides d₂-5hmC and d₃-5mC were added, followed by centrifugation of the sample (12,100g, 15 min). Each sample was performed at least in duplicate with independent concentrations of the two labeled nucleosides. The concentrations of standard solutions were chosen to be in the expected range of the sample nucleoside concentration.

LC-MS

The samples (100 μ L injection volume) were analyzed by LC-MS on a Thermo Finnigan LTQ Orbitrap XL and were chromatographed by a Dionex Ultimate 3000 HPLC system with a flow of 0.15 mL/min over an Uptisphere120-3HDO column from Interchim. The column temperature was maintained at 30°C. Eluting buffers were buffer C (2 mM HCOONH₄ in H₂O (pH 5.5)) and buffer D (2 mM HCOONH₄ in H₂O/MeCN 20/80 (pH 5.5)). The gradient was 0 \rightarrow 12 min; 0% \rightarrow 3% buffer D; 12 \rightarrow 60 min; 3% \rightarrow 60% buffer D; 60 \rightarrow 62 min; 60% \rightarrow 100% buffer D; 62 \rightarrow 70 min; 100% buffer D; 70 \rightarrow 85 min; 100 \rightarrow 0% buffer D; 85 \rightarrow 95 min; 0 % buffer D. The elution was monitored at 260 nm (Dionex Ultimate 3000 Diode Array Detector). The chromatographic eluent was directly injected into the ion source without prior splitting. Ions were scanned by the use of a positive polarity mode over a full-scan range of m/z 200–1,000 with a resolution of 30,000. Parameters of the mass spectrometer were tuned with a freshly mixed solution of adenosine (5 μ M) in buffer C. The parameters used in this section were sheath gas flow rate, 16 arb; auxiliary gas flow rate, 11 arb; sweep gas flow rate, 4 arb; spray voltage, 5.0 kV; capillary temperature, 200°C; capillary voltage, 12 V, tube lens 86 V.

Pyrosequencing of DNA

To confirm IDH1 mutations detected by IHC staining, we sequenced a 88 bp long fragment of the IDH1 gene including codon 132. The IDH1 primers were designed using PSQ Assay design software (Qiagen, Hilden, Germany). As forward primer, we used 5'-biotin-AAAAATATCCCCCG GCTTG-3' and as reverse primer 5'-TGCCAACATGACTTA CTTGATCC-3'. PCR reactions were performed using the HotStarTaq DNA polymerase master mix (Qiagen, Hilden, Germany) according to the manufacturer's protocol and a

standard PCR protocol. The PCR product was then sequenced using a PyroMark Q24 System (Qiagen, Hilden, Germany) and the Pyro Gold reagent kit (Qiagen, Hilden, Germany). We used 5'-TGATCCCCATAAGCAT-3' as sequencing primer. The subsequent processing was performed according to the manufacturer's protocols. Data analysis was performed using PyroMark Q24 software (Qiagen, Hilden, Germany).

Statistical analysis

Statistical calculations were performed using ANOVA single factor analysis and Tukey-Kramer *post hoc* test as well as unpaired *t*-test. Analysis was performed using GraphPad Prism 5.

Results

Not all cells express 5hmC in normal human brain and brain tumors at detectable levels

IHC with an antibody against 5hmC in general showed either strong staining or no staining with only a small number of faintly stained nuclei (Fig. 1). In normal human frontal brain, the majority of neurons of the cortex showed strong reactivity for 5hmC (Fig. 1a, upper right corner). In contrast, there was weaker immunohistochemical staining for 5hmC in the frontal subcortical white matter (Fig. 1a, lower left corner). About 70% of WM cells showed negative staining; these cells had mostly round, small nuclei and appeared to be oligodendrocytes. In the occipital cortex (Fig. 1b) and subcortical white matter (Fig. 1c), we found comparable results. In human brain tumors, we found significantly lower numbers of 5hmC positive cells. In astrocytomas and GBMs (Figs. 1d–1g), the number of 5hmC positive cells decreased from pilocytic astrocytomas (Fig. 1d) to diffuse astrocytomas (Fig. 1e), AAs (Fig. 1f) and GBMs with mean of 1.43% positive cells (Fig. 1g). Whilst there were about 10% of positive cells in pilocytic astrocytomas, GBMs showed only very few positive cells. In ependymomas (Figs. 1h–1j), we found that most of the cells were not stained. Grade I ependymomas (Fig. 1h) showed more 5hmC positive cells than Grade II (Fig. 1i) and Grade III tumors (Fig. 1j). Grades II and III ependymomas showed more or less equal staining but anaplastic ependymomas showed a weaker staining for 5hmC. Furthermore, there were strong regional variations. In meningiomas (Figs. 1k–1l), we found similar results to ependymomas. Grade I meningiomas (Fig. 1k) showed more 5hmC positive cells than Grade II tumors (Fig. 1l) and Grade II meningiomas showed a weaker staining for 5hmC with regional variations. We found that staining for 5hmC and the proliferation-associated Ki-67 was mutually exclusive; an example of this general finding is shown in Figures 1m–1o. We often observed a rhythmic variation of areas with higher proliferative activity (Ki-67) and sparse 5hmC staining and *vice versa*.

There are significantly more 5hmC positive stained cells in the cortex compared to white matter areas. 5hmC/dG in human brain is significantly higher in cortex than white matter

When we counted the 5hmC positive and negative cells the values for various cortical areas did not show significant differences (Fig. 2a, $p > 0.05$, ANOVA and Tukey-Kramer *post hoc* test). Furthermore, we did not find any significant difference in the ration of 5hmC positive cells in various white matter areas (Fig. 2a, $p > 0.05$, ANOVA and Tukey-Kramer *post hoc* test). However, we found significant differences comparing frontal cortex and frontal white matter areas (Fig. 2a, $p < 0.01$, ANOVA and Tukey-Kramer *post hoc* test) as well as occipital cortex and occipital white matter areas (Fig. 2a, $p < 0.05$, ANOVA and Tukey-Kramer *post hoc* test).

Additionally, we performed LC-MS measurements. 5hmC was found in measurable amounts in all brain regions but there was no significant difference between various cortical (Fig. 2b, $p > 0.05$, ANOVA and Tukey-Kramer *post hoc* test) and various white matter areas (Fig. 2b, $p > 0.05$, ANOVA and Tukey-Kramer *post hoc* test). But the values measured in the frontal cortex were significantly higher than in the frontal white matter (Fig. 2b, $p < 0.01$, ANOVA and Tukey-Kramer *post hoc* test) and the values measured in the occipital cortex were significantly higher than in the occipital white matter (Fig. 2b, $p < 0.001$, ANOVA and Tukey-Kramer *post hoc* test).

The 5mC values measured by LC-MS did not show significant differences between different cortical areas ($p > 0.05$ using ANOVA and Tukey-Kramer *post hoc* test, Fig. 2c) nor between different white matter areas ($p > 0.05$ using ANOVA and Tukey-Kramer *post hoc* test, Fig. 2c) but we found significant differences between cortical and white matter areas ($p < 0.05$, ANOVA and Tukey-Kramer *post hoc* test, Fig. 2c).

The number of 5hmC positive cells and 5hmC/dG levels in human brain tumors are related to WHO grade

One hundred seventeen human tumors were selected for analysis including 6 pilocytic astrocytomas (Grade I), 13 diffuse astrocytomas (Grade II), 18 AAs (Grade III) and 43 GBMs (Grade IV), 10 ependymomas Grade I, 9 ependymomas (Grade II) and 4 anaplastic ependymomas (Grade III), 6 WHO Grade I meningiomas and 8 atypical meningiomas (Grade II).

In WHO Grade I tumors, the mean of 5hmC positive cells was 16.73%, in Grade II 7.87%, in Grade III 5.51% and in Grade IV 1.07% (Fig. 2d) with a highly significant difference between Grades I and II ($p < 0.001$, ANOVA and Tukey-Kramer *post hoc* test), Grades I and III ($p < 0.001$, ANOVA and Tukey-Kramer *post hoc* test), Grades I and IV ($p < 0.001$, ANOVA and Tukey-Kramer *post hoc* test) as well as Grades II and IV ($p < 0.001$, ANOVA and Tukey-Kramer *post hoc* test).

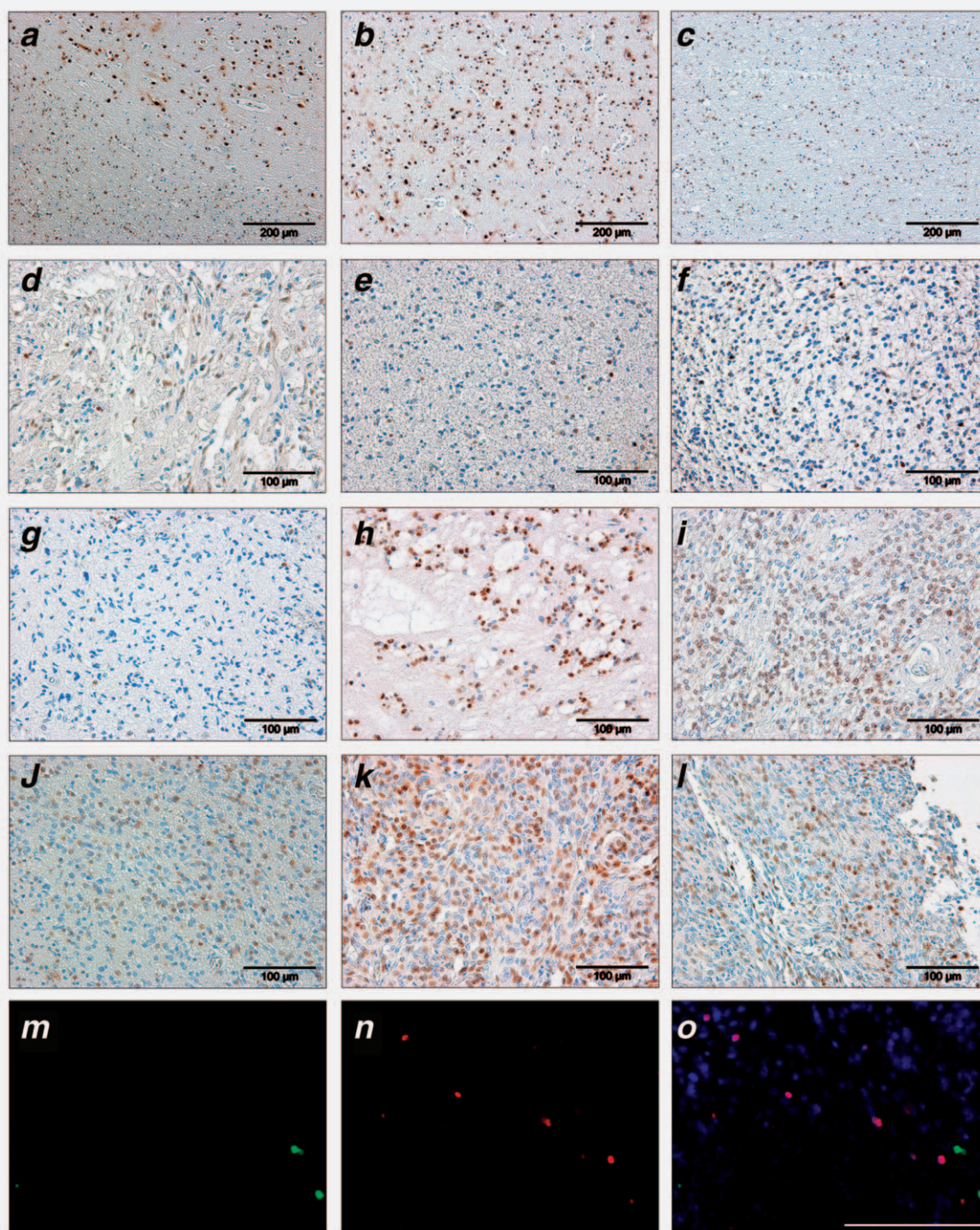


Figure 1. IHC with an antibody against 5hmC. (a) In the normal frontal lobe we see differences in staining of the cortex and subcortical white matter. In the cortex (upper right corner) there are numerous clearly visible positively stained neurons. In the subcortical white matter (lower left corner) there is diminished staining for 5hmC, but distinct positively stained cells are seen surrounded by negative ones. (b) In the normal occipital cortex, there is a clear staining of the majority (about 60%) of cells. (c) In normal occipital white matter, there are fewer 5hmC positive cells (about 30%) compared to the occipital cortex. (d) In human pilocytic astrocytomas (WHO Grade I) the majority of tumor cells are negative, only about 10% of tumor cells stain positive. (e) In diffuse astrocytomas less than 5% of cells stain positive for 5hmC. (f) AAs show lower values of 5hmC positive cells compared to low-grade gliomas. (g) GBMs show only very low positive staining for 5hmC. (h) In Grade I ependymomas most cells stain negative for 5hmC. (i) Ependymomas Grade II show lower numbers of 5hmC positive cells than Grade I tumors with a large intratumoral variation. (j) Anaplastic ependymomas show almost the same number of 5hmC positive cells compared to Grade II ependymomas but the cells stain much weaker. Furthermore there is a large intratumoral variation. (k) In Grade I meningiomas we see only a minority of positively stained cells with a large intratumoral variation. (l) Meningiomas Grade II show fewer 5hmC positive cells than Grade I tumors and the cells seem to stain more weakly than in Grade I tumors with large intratumoral variations. (m–o) Immunofluorescence staining of a GBM with antibodies against 5hmC (m), the proliferation marker Ki-67 (n) and DAPI. Scale bar is 100 μm. Cells stained positive for Ki-67 show no detectable signal for 5hmC in the merge picture (o).

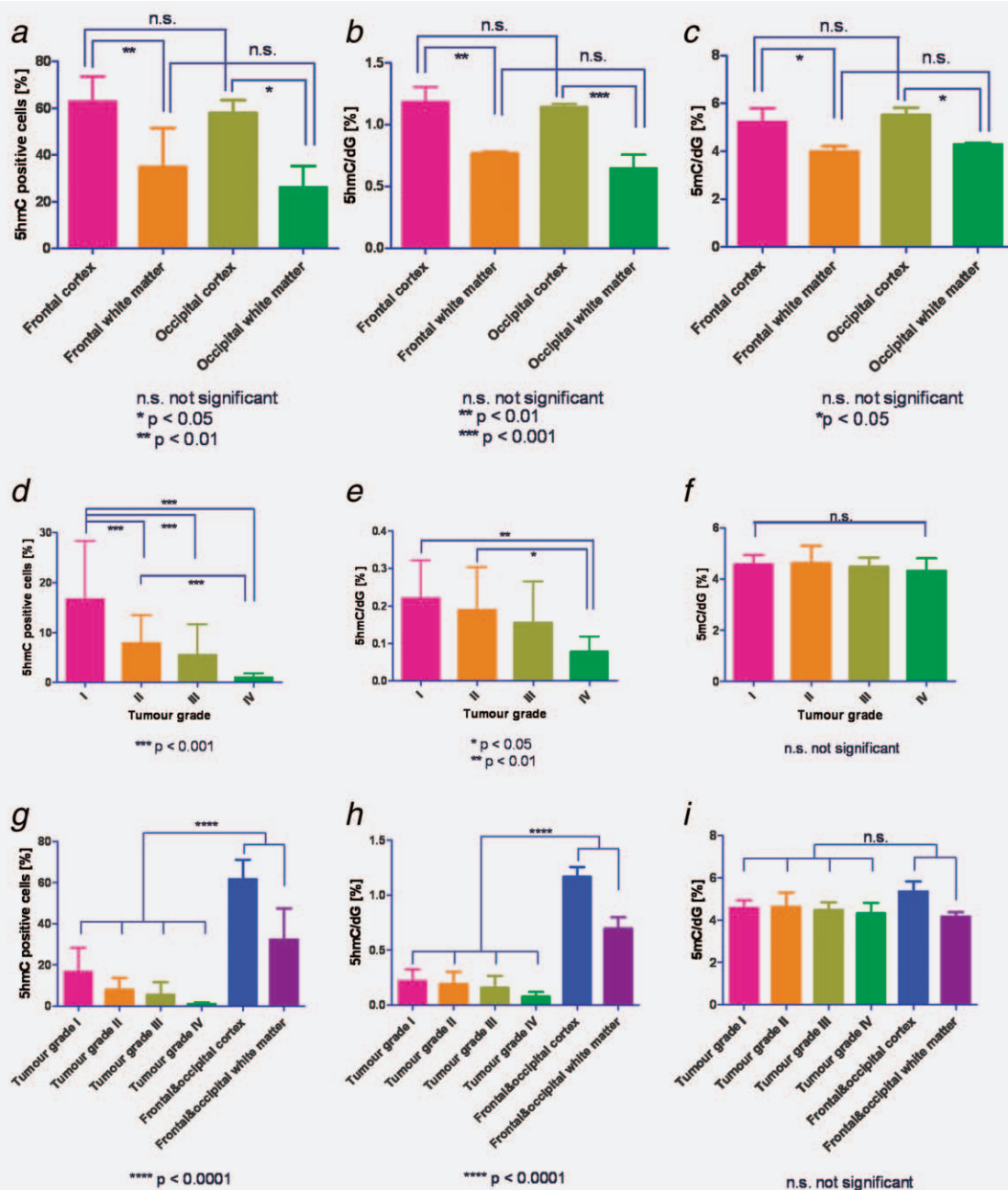


Figure 2. Percentage of 5hmC positive cells and LC-MS values of 5hmC and 5mC in normal human brain and in brain tumors. Indicated are the mean and SD. (a) There was no significant differences of 5hmC positive cells in various white matter areas as well as in various cortex regions of the human brain ($p > 0.05$, ANOVA and Tukey–Kramer *post hoc* test) but there were highly significant differences in the cortex compared to the white matter ($p < 0.01$ in case of frontal cortex and frontal white matter and $p < 0.05$ in case of occipital cortex and occipital white matter, ANOVA and Tukey–Kramer *post hoc* test). (b) LC-MS values showed no significant difference between various white matter regions and between various cortex regions ($p > 0.05$, ANOVA and Tukey–Kramer *post hoc* test) but highly significant differences between cortex and white matter regions ($p < 0.01$ in case of frontal cortex and frontal white matter and $p < 0.001$ in case of occipital cortex and occipital white matter, ANOVA and Tukey–Kramer *post hoc* test). (c) The distribution of 5mC in different brain regions showed no significant difference between different cortical regions as well as in different white matter regions ($p > 0.05$, ANOVA and Tukey–Kramer *post hoc* test) but there were significant difference between cortical and white matter regions ($p < 0.05$, ANOVA and Tukey–Kramer *post hoc* test). (d) A comparison of 5hmC positive cells in human brain tumors showed highly significant differences between Grade I and Grade II tumors ($p < 0.001$, ANOVA and Tukey–Kramer *post hoc* test), Grade I and Grade III tumors ($p < 0.001$, ANOVA and Tukey–Kramer *post hoc* test), Grade I and Grade IV tumors ($p < 0.001$, ANOVA and Tukey–Kramer *post hoc* test) as well as Grade II and Grade IV tumors ($p < 0.001$, ANOVA and Tukey–Kramer *post hoc* test). (e) In LC-MS we found significant lower amounts of 5hmC in Grade I compared to Grade IV tumors ($p < 0.01$, ANOVA and Tukey–Kramer *post hoc* test). (f) The 5mC values did not show a correlation with tumor grade ($p > 0.05$, ANOVA and Tukey–Kramer *post hoc* test). (g) A comparison of tumors with normal brain showed highly significantly lower numbers of 5hmC positive cells in tumors compared to normal brain ($p < 0.0001$, unpaired *t*-test). (h) In LC-MS we found that tumors show significant higher amount of 5hmC compared to normal brain ($p < 0.0001$, unpaired *t*-test). (i) There was no significant difference between tumor and normal brain in regard to 5mC ($p > 0.05$, unpaired *t*-test). [Color figure can be viewed in the online issue, which is available at wileyonlinelibrary.com.]

By mass spectrometry we see that in Grade I tumors the 5hmC values were 0.22% 5hmC/dG, in Grade II 0.19% 5hmC/dG, in Grade III 0.16% 5hmC/dG and in Grade IV 0.078% 5hmC/dG with a significant difference between Grades I and IV tumors ($p < 0.01$, ANOVA and Tukey–Kramer *post hoc* test) as well as Grades II and IV tumors ($p < 0.05$, ANOVA and Tukey–Kramer *post hoc* test) (Fig. 2e).

No such relation was found in LC-MS measurements of 5mC in WHO tumor grades (Fig. 2f). Grade I tumors showed mean values of 4.58% 5mC/dG, Grade II 4.62% 5mC/dG, Grade III 4.47% 5mC/dG and Grade IV 4.32% 5mC/dG with no significant difference between different tumor grades ($p > 0.05$, ANOVA and Tukey–Kramer *post hoc* test).

The number of 5hmC positive cells identified in brain tumors was significantly lower compared to normal cortex and white matter (Fig. 2g). While in normal human brain mean number of 5hmC positive cells was 61.48% in the cortex and 32.39% in the white matter, the mean in tumor tissue was 6.58% ($p < 0.0001$, unpaired *t*-test).

These data were paralleled by LC-MS (Fig. 2h). In normal cortex, we measured 1.17% 5hmC/dG, in the white matter 0.70% 5hmC/dG and in tumor tissue the average value was 0.16% 5hmC/dG ($p < 0.0001$, unpaired *t*-test).

As regards 5mC no significant difference was observed between normal brain tissue and tumor (Fig. 2i) with a mean of 4.85% 5mC/dG in the normal human brain and 4.50% 5mC/dG in tumors ($p > 0.05$, unpaired *t*-test).

When tumors were grouped according to their cellular lineages, we obtained similar differences of 5hmC related to the tumor grade.

In astrocytomas, the mean of 5hmC positive stained cells was 8.91% in Grade I pilocytic astrocytomas, 4.40% in Grade II diffuse astrocytomas, 3.34% in Grade III AAs and 1.07% in Grade IV GBMs (Fig. 3a) with highly significant differences between Grade I and Grade III tumors ($p < 0.001$, ANOVA and Tukey–Kramer *post hoc* test), Grade I and Grade IV tumors ($p < 0.001$, ANOVA and Tukey–Kramer *post hoc* test) and Grade II and Grade IV tumors ($p < 0.001$, ANOVA and Tukey–Kramer *post hoc* test) as well as significant differences between Grade I and Grade II tumors ($p < 0.01$, ANOVA and Tukey–Kramer *post hoc* test) and Grade III and Grade IV tumors ($p < 0.01$, ANOVA and Tukey–Kramer *post hoc* test) (Fig. 3a).

Using LC-MS, we found mean values of 0.19% 5hmC/dG in Grade I astrocytomas, 0.24% 5hmC/dG in Grade II, 0.13% 5hmC/dG in Grade III and 0.078% 5hmC/dG in Grade IV tumors (Fig. 3b) with significant differences between Grade II and Grade IV tumors ($p < 0.01$, ANOVA and Tukey–Kramer *post hoc* test) (Fig. 3b).

In regard to 5mC, there were no significant differences related to WHO grades of astrocytic gliomas using LC-MS (Fig. 3c). The mean value of Grade I astrocytomas was 4.68% 5mC/dG, of Grade II 4.82% 5mC/dG, of Grade III 4.36% 5mC/dG and of Grade IV 4.32% 5mC/dG ($p > 0.05$, ANOVA and Tukey–Kramer *post hoc* test) (Fig. 3c).

In ependymal tumors, we found a tendency of 5hmC positive cells between Grade I as well as Grade II and Grade III tumors by IHC staining but we did not find significant differences ($p > 0.05$, ANOVA and Tukey–Kramer *post hoc* test) (Fig. 3d). Grade I ependymomas showed mean values of 21.62% positive stained cells, Grade II and Grade III tumors show almost equal values of 5hmC positively stained cells (12.47% and 13.12%).

LC-MS measurements showed that WHO Grade I ependymomas have mean values of 0.286% 5hmC/dG, Grade II ependymomas 0.197% 5hmC/dG and anaplastic ependymomas (WHO Grade III) 0.193% 5hmC/dG and thus paralleled the same tendency as the immunohistochemical stainings ($p > 0.05$, ANOVA and Tukey–Kramer *post hoc* test) (Fig. 3e).

With regard to 5mC no significant differences were found using LC-MS; in Grade I ependymomas the mean was 4.70% 5mC/dG, in Grade II 4.73% 5mC/dG and in Grade III 4.65% 5mC/dG ($p > 0.05$, ANOVA and Tukey–Kramer *post hoc* test) (Fig. 3f).

A comparison of WHO Grades I and II meningiomas in IHC showed lower numbers of 5hmC positive cells in Grade II meningiomas compared to Grade I meningiomas (mean of 18.05% positive cells in Grade I and 6.51% positive cells in Grade II) but the difference did not reach statistical significance ($p > 0.05$, unpaired *t*-test) (Fig. 3g).

By mass spectrometry, we found a mean value of 0.163% 5hmC/dG in Grade I and 0.140% 5hmC/dG in one Grade II atypical meningioma, which again paralleled the same tendency as in IHC but this did not reach statistical significance ($p > 0.05$, unpaired *t*-test) (Fig. 3h).

Again, 5mC/dG levels did not show significant differences between Grade I and Grade II meningiomas (4.20% 5mC/dG in Grade I meningiomas and 4.32% 5mC/dG in Grade II meningiomas, $p > 0.05$, unpaired *t*-test) (Fig. 3i).

The number of 5hmC positive cells is significantly related to IDH1 mutations in diffuse and anaplastic astrocytomas but not in glioblastomas

Additionally, we analyzed the IDH1 status of all astroglial tumors by IHC using an IDH1^{R132H} antibody and pyrosequencing of the IDH1 gene. As expected we did not find IDH1 mutations in pilocytic astrocytomas (0% mutated IDH1), but we found 7 IDH1 mutations in diffuse astrocytomas (54% mutated IDH1), 9 IDH1 mutations in AAs (50% mutated IDH1) and 11 IDH1 mutations in GBMs (26% mutated IDH1).

Comparing 5hmC positive cells of diffuse and AAs as well as in GBMs (Fig. 4a) we found highly significant differences between diffuse astrocytomas with and without IDH1 mutation (1.50% 5hmC positive cells in tumors with IDH1 mutation compared to 7.31% 5hmC positive cells in tumors without IDH1 mutation, $p < 0.001$, ANOVA and Tukey–Kramer *post hoc* test) and significant differences in AAs with and without IDH1 mutation (1.80% 5hmC positive cells in tumors with IDH1 mutation and 4.87% 5hmC positive cells in tumors without IDH1 mutation, $p < 0.01$, ANOVA and Tukey–Kramer *post hoc* test). In GBM, we did not find significant differences

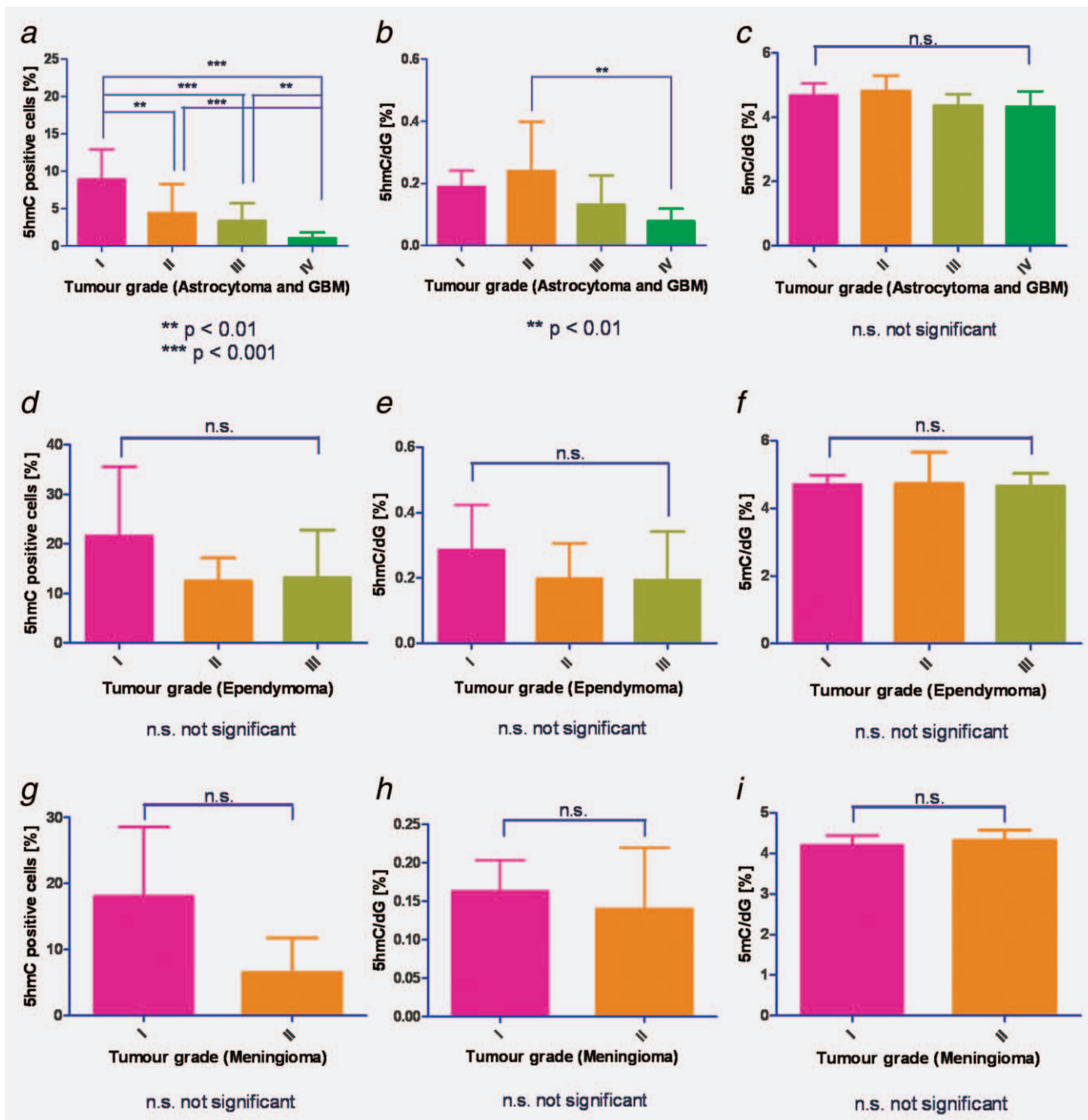


Figure 3. Percentage of 5hmC positive cells and LC-MS values of 5hmC and 5mC in various tumor entities. Indicated are the mean and SD. (a) In astrocytomas and GBMs a good correlation between the number of 5hmC positive cells and tumor grade was seen. Pilocytic Grade I astrocytomas showed highly significantly higher numbers of 5hmC positive cells compared to Grade III tumors ($p < 0.001$, ANOVA and Tukey–Kramer *post hoc* test) and Grade IV tumors ($p < 0.001$, ANOVA and Tukey–Kramer *post hoc* test), and Grade II tumors showed highly significant higher numbers of 5hmC positive cells compared to Grade IV GBM ($p < 0.001$, ANOVA and Tukey–Kramer *post hoc* test). Furthermore Grade I astrocytomas showed significantly lower numbers of 5hmC positive cells compared to Grade II tumors ($p < 0.01$, ANOVA and Tukey–Kramer *post hoc* test) as well as Grade III tumors showed significantly lower numbers of 5hmC positive cells compared to Grade IV GBM ($p < 0.01$, ANOVA and Tukey–Kramer *post hoc* test). (b) LC-MS showed similar results. Diffuse Grade II astrocytomas showed significantly higher amounts of 5hmC compared to undifferentiated Grade IV GBMs ($p < 0.01$, ANOVA and Tukey–Kramer *post hoc* test). (c) 5mC showed no significant differences between different tumor grades ($p > 0.05$, ANOVA and Tukey–Kramer *post hoc* test). (d) Using IHC, in ependymomas Grade I there were more 5hmC positive cells than in ependymomas Grades II and III, but there was no significant decrease ($p > 0.05$, ANOVA and Tukey–Kramer *post hoc* test). (e) Using LC-MS we found higher amounts of 5hmC in Grade I ependymomas compared to Grades II and III tumors without statistical significance ($p > 0.05$, ANOVA and Tukey–Kramer *post hoc* test). (f) 5mC showed no significant differences in ependymomas of different WHO grades ($p > 0.05$, ANOVA and Tukey–Kramer *post hoc* test). (g) Meningiomas showed a decrease of 5hmC positive cells in Grade II tumors compared to Grade I tumors but the difference did not reach statistical significance ($p > 0.05$, unpaired *t*-test). (h) LC-MS showed higher amounts of 5hmC in Grade I tumors compared to Grade II tumors without statistical significance ($p > 0.05$, unpaired *t*-test). (i) The amount of 5mC did not show any significant differences in regard to tumor grade ($p > 0.05$, unpaired *t*-test) [Color figure can be viewed in the online issue, which is available at wileyonlinelibrary.com.].

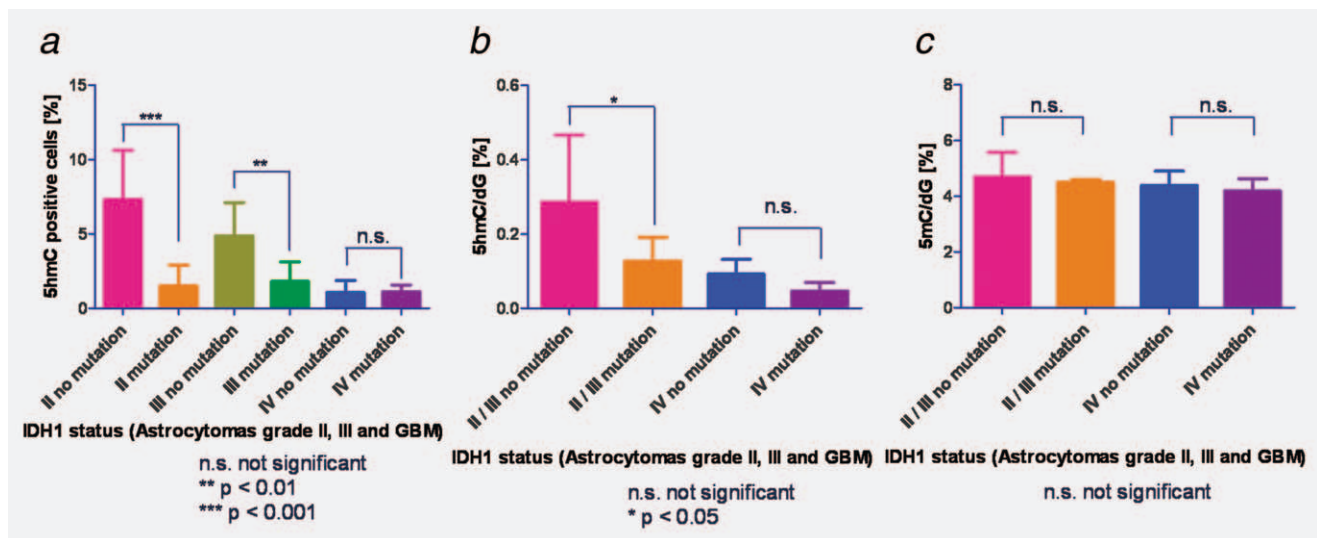


Figure 4. Number of 5hmC positive cells and LC-MS values of 5hmC/dG and 5mC/dG in astrocytomas and GBMs with regard to IDH1 status. Indicated are the mean and SD. (a) Comparing the number of 5hmC positive cells in diffuse and AAs as well as in GBMs with and without IDH1 mutations we found that diffuse astrocytomas without IDH1 mutation had significantly more 5hmC positive cells ($p < 0.001$, ANOVA and Tukey–Kramer *post hoc* test). Similar and highly significant differences were noted between AAs with and without IDH1 mutation ($p < 0.01$, ANOVA and Tukey–Kramer *post hoc* test). GBMs with and without IDH1 mutation did not show significant differences in the number of 5hmC positive cells ($p > 0.05$, ANOVA and Tukey–Kramer *post hoc* test). Remarkably, Grade II diffuse and Grade III AAs that had a IDH1 mutation and GBMs with and without mutation had very low 5hmC counts, which were not significantly different between these groups ($p > 0.05$). (b) Using MS-LC we could parallel these results with significant differences between Grades II and III astrocytomas with and without mutant IDH1 ($p < 0.05$, ANOVA and Tukey–Kramer *post hoc* test). There was no significant difference in GBMs with and without IDH1 mutation ($p > 0.05$, ANOVA and Tukey–Kramer *post hoc* test). (c) The amount of 5mC did not show any significant differences in regard to IDH1 mutations ($p > 0.05$, ANOVA and Tukey–Kramer *post hoc* test). [Color figure can be viewed in the online issue, which is available at wileyonlinelibrary.com.]

between tumors with or without IDH1 mutation ($p > 0.05$, ANOVA and Tukey–Kramer *post hoc* test) (Fig. 4a).

By mass spectrometry, we found a mean value of 0.287% 5hmC/dG in Grade II and Grade III tumors without IDH1 mutation and 0.127% 5hmC/dG in tumors with IDH1 mutation with a significant difference ($p < 0.05$, ANOVA and Tukey–Kramer *post hoc* test) (Fig. 4b). In GBM, we did not find significant differences between tumors with or without IDH1 mutation ($p > 0.05$, ANOVA and Tukey–Kramer *post hoc* test) (Fig. 4b).

We did not find significant differences in the amount of 5mC/dG between Grades II and III astrocytomas with and without IDH1 mutation as well as GBMs (4.69% 5mC/dG in Grades II and III tumors without IDH1 mutation and 4.50% 5hmC/dG in tumors with IDH1 mutation, $p > 0.05$, ANOVA and Tukey–Kramer *post hoc* test, and 4.38% 5hmC/dG in GBMs without IDH1 mutation and 4.19% 5hmC/dG with IDH1 mutation, $p > 0.05$, ANOVA and Tukey–Kramer *post hoc* test) (Fig. 4c).

Discussion

The profoundly distorted epigenetic landscape of tumor cells is only beginning to emerge.^{12–14} DNA methylation, a major epigenetic mechanism of gene silencing, seems to play a major role in tumor pathogenesis. Transcriptional inactivation caused by promoter hypermethylation affects genes

involved in the main cellular pathways, DNA repair, vitamin response, Ras signaling, cell-cycle control, p53 network and apoptosis.¹⁵ Hypermethylation patterns are tumor-type specific and it is still unclear why certain regions become hypermethylated, whereas others remain unmethylated. Hypomethylation at specific promoters can activate the aberrant expression of oncogenes and induce loss of imprinting.¹⁴

DNA methylation is mediated by the DNMT family of enzymes that catalyze the transfer of a methyl group from S-adenosyl methionine to DNA. However, it seems that the DNA methylome is reprogrammed during development and we hypothesized that this might also be the case in gliomas. The discovery that 5mC can be oxidized to 5hmC by the action of the TET enzymes has engendered ideas of a role of TET and 5hmC in genetic reprogramming, *i.e.*, that 5hmC could be an intermediate leading to demethylation of 5mC and consequently a reversal of gene silencing by methylation. Indeed, very recent research has shown that TET proteins can convert 5mC to 5-formylcytosine and 5-carboxylcytosine and that the latter can be excised by thymine-DNA glycosylase (TDG), which has been interpreted as a pathway for active DNA demethylation.^{5–7}

The results presented here show that hydroxymethylation of genomic DNA cytidine residues is a feature found in the human central nervous system (CNS). The highest values were found in cortical areas (mean 1.17% 5hmC/dG) while

the white matter showed much lower values of 0.696% 5hmC/dG (ratio 1.68:1). Since neurons in the cortex are outnumbered by glia cells by a factor of 2–10 and IHC did not show a difference in the percentage of glial nuclei in the cortex and WM, we have to assume that the values of 5hmC/dG in neurons must be even higher. Percentage values of 5hmC/dG in the human adult cortex are the highest values published to date. The values of 5mC were around 5.3% of dG in the cerebral cortex and 4.2% in the cerebral white matter (ratio 1.26:1). Thus, overall it seems that a higher percentage of DNA is hydroxymethylated in neurons in absolute terms but also in relation to 5mC.

By comparison in the adult mouse, 5hmC/dG levels were highest in the CNS¹⁶; the adult murine cerebral cortex and hippocampus showed values around 0.6% 5hmC/dG while in other organs such as the kidney, heart and lung values were around 0.15%–0.2% and even lower in the liver, spleen and testis. Remarkably, 5mC/dG percentages were around 4.5% in most organs¹⁶ and various areas of the brain.¹⁷ Using an immunoprecipitation technique Jin *et al.* reported that 5hmC in DNA from human frontal lobe was more selectively targeted to genes than was 5mC and was particularly enriched at promoters and in intragenic regions. The presence of 5hmC was more positively correlated with gene expression than was the presence of 5mC.¹⁸

Surprisingly, our immunohistochemical results demonstrate that 5hmC is quite unevenly distributed in cells of neuronal and glial lineage. We would not conclude from our data that DNA in some cells is free of 5hmC, but our results unequivocally show that there is a wide variation in cellular 5hmC concentration.

In our investigation, 5hmC values in gliomas range from 0.086% to 0.24% 5hmC/dG and thus are surprisingly low when compared to measurements in the white matter. 5mC/dG values in tumors were around 4.5% and thus were slightly higher than in normal white matter. Since tumor infiltration areas could be a possible confounding factor that is difficult to exclude in investigating gliomas, we took great care to sample pure tumor areas excluding infiltration zones of the white matter or cortex as far as that is possible on light-microscopic inspection. However, tumor infiltration may still not be a totally negligible factor. When all tumor entities including astrocytomas, ependymomas and meningiomas were grouped by WHO grade, significantly lower 5hmC/dG values were noted in high-grade anaplastic tumors than in low-grade tumors while no significant differences were found in 5mC/dG values. When considering 5hmC/dG values of the individual tumor lineages, significant differences were found for low-grade astrocytomas *versus* GBMs, whereas only a tendency could be shown regarding ependymomas and meningiomas. Again, as in the normal brain, IHC demonstrated uneven cellular distribution in various tumor cell populations. We found that staining for 5hmC and the proliferation-associated Ki-67 was mutually exclusive and often observed a rhythmic variation of areas with higher proliferative activity (Ki-67) and sparse 5hmC staining and *vice*

versa. Again, 5mC/dG measurements showed no significant differences between WHO low- and high-grade tumors.

Thus by using LC-MS we have shown that 5hmC values related to the number of dG in the human brain are highest in gray matter areas, considerably lower in the white matter and even lower in brain tumors. Comparable values of 5hmC in the prefrontal cortex and a similar reduction in astrocytomas have recently been published by Jin *et al.*¹⁹; data on the white matter, GBMs and other brain tumors are not available at present. In the tumor group, lower 5hmC values were associated with anaplasia (WHO Grade IV), *i.e.*, a low degree of cellular differentiation and high mitotic activity. IHC with an antibody against 5hmC, more precisely the ratio of positively stained nuclei related to unstained nuclei, showed the same tendency as LC-MS; higher values were measured in the gray matter *vs.* white matter and highly differentiated tumors *vs.* anaplastic tumors. Additional factors such as the different cells of origin of these tumors may influence the 5hmC values. Pilocytic astrocytomas may be a particular case in point since they are known to be genetically different from higher-grade astrocytomas.

Acute myeloid leukemia (AML)-associated mutations of IDH1 and IDH2 that display a neomorphic enzyme activity resulting in the production of 2-hydroxyglutarate (2HG) have been shown to impair the catalytic function of TET2, an α -ketoglutarate (2-oxoglutarate or 2OG)-dependent enzyme.²⁰ Xu *et al.* reported decreased 5hmC values in a mixture of Grade III astrocytomas and GBMs harboring mutant IDH1.²¹ Similarly our data show in greater depth a significant difference in the percentage of 5hmC positive cells in diffuse and AAs with and without IDH1 mutation but not in GBMs (Fig. 4a). LC-MS measurements showed the same relationship between diffuse and AAs with and without IDH1 mutation and in GBMs.

Jin *et al.* found 5hmC levels were independent of IDH1 mutations in their sample of gliomas¹⁹; their data showed the same tendency as ours but did not reach statistical significance.

In a cohort of patients with AML, IDH1/2 mutations and TET2 loss-of-function mutations were mutually exclusive and elicited similar epigenetic defects.²⁰ Kim *et al.* found no TET2 mutation in 29 low-grade diffuse gliomas,²² neither have we identified TET2 loss-of function mutations in seven investigated cases of astrocytomas and GBMs (data not shown). Thus, concluding from what we know from myeloid leukemia, in human gliomas the observed very low 5hmC values may be related to functional impairment of the TET enzymes by 2HG. Remarkably, Grade II diffuse and Grade III AAs and GBMs that had IDH1 mutations had almost identical low 5hmC values. GBMs with no IDH1 mutation, which by and large are primary GBMs, had equally low values; therefore other, unknown factors may impair 5mC oxidation in these tumors.

Acknowledgements

The authors thank the Brain Bank Munich (Sigrun Roeber) for providing control tissues as well as Virginie Guibourt and Michael Schmidt for expert technical assistance. M. Mün. and T.P. thank the Fonds der Chemischen Industrie for pre-doctoral fellowships.

References

- Hegi ME, Diserens AC, Gorlia T, Hamou MF, de Tribolet N, Weller M, Kros JM, Hainfellner JA, Mason W, Mariani L, Bromberg JE, Hau P, et al. MGMT gene silencing and benefit from temozolomide in glioblastoma. *N Engl J Med* 2005;352:997–1003.
- Wick W, Hartmann C, Engel C, Stoffels M, Felsberg J, Stockhammer F, Sabel MC, Koeppen S, Ketter R, Meyermann R, Rapp M, Meisner C, et al. NOA-04 randomized phase III trial of sequential radiochemotherapy of anaplastic glioma with procarbazine, lomustine, and vincristine or temozolomide. *J Clin Oncol* 2009;27:5874–80.
- Kaina B, Christmann M, Naumann S, Roos WP. MGMT: key node in the battle against genotoxicity, carcinogenicity and apoptosis induced by alkylating agents. *DNA Repair (Amst)* 2007;6:1079–99.
- Kriaucionis S, Heintz N. The nuclear DNA base 5-hydroxymethylcytosine is present in Purkinje neurons and the brain. *Science* 2009;324:929–30.
- He YF, Li BZ, Li Z, Liu P, Wang Y, Tang Q, Ding J, Jia Y, Chen Z, Li L, Sun Y, Li X, et al. Tet-mediated formation of 5-carboxylcytosine and its excision by TDG in mammalian DNA. *Science* 2011;333:1303–7.
- Ito S, Shen L, Dai Q, Wu SC, Collins LB, Swenberg JA, He C, Zhang Y. Tet proteins can convert 5-methylcytosine to 5-formylcytosine and 5-carboxylcytosine. *Science* 2011;333:1300–3.
- Pfaffeneder T, Hackner B, Truss M, Munzel M, Muller M, Deiml CA, Hagemeier C, Carell T. The discovery of 5-formylcytosine in embryonic stem cell DNA. *Angew Chem Int Ed Engl* 2011;50:7008–12.
- Tahiliani M, Koh KP, Shen Y, Pastor WA, Bandukwala H, Brudno Y, Agarwal S, Iyer LM, Liu DR, Aravind L, Rao A. Conversion of 5-methylcytosine to 5-hydroxymethylcytosine in mammalian DNA by MLL partner TET1. *Science* 2009;324:930–5.
- Koh KP, Yabuuchi A, Rao S, Huang Y, Cunliffe K, Nardone J, Laiho A, Tahiliani M, Sommer CA, Mostoslavsky G, Lahesmaa R, Orkin SH, et al. Tet1 and Tet2 regulate 5-hydroxymethylcytosine production and cell lineage specification in mouse embryonic stem cells. *Cell Stem Cell* 2011;8:200–13.
- Haffner MC, Chaux A, Meeker AK, Esopi DM, Gerber J, Pellakuru LG, Toubaji A, Argani P, Iacobuzio-Donahue C, Nelson WG, Netto GJ, De Marzo AM, et al. Global 5-hydroxymethylcytosine content is significantly reduced in tissue stem/progenitor cell compartments and in human cancers. *Oncotarget* 2011;2:627–37.
- Louis DN, Ohgaki H, Wiestler OD, Cavenee WK, Burger PC, Jouvet A, Scheithauer BW, Kleihues P. The 2007 WHO classification of tumours of the central nervous system. *Acta Neuropathol* 2007;114:97–109.
- Esteller M. Cancer epigenomics: DNA methylomes and histone-modification maps. *Nat Rev Genet* 2007;8:286–98.
- Sharma S, Kelly TK, Jones PA. Epigenetics in cancer. *Carcinogenesis* 2009;31:27–36.
- Portela A, Esteller M. Epigenetic modifications and human disease. *Nat Biotechnol* 2010;28:1057–68.
- Esteller M. Epigenetic gene silencing in cancer: the DNA hypermethylome. *Hum Mol Genet* 2007;16 Spec No 1:R50–9.
- Globisch D, Munzel M, Muller M, Michalakakis S, Wagner M, Koch S, Bruckl T, Biel M, Carell T. Tissue distribution of 5-hydroxymethylcytosine and search for active demethylation intermediates. *PLoS One* 2010;5:e15367.
- Munzel M, Globisch D, Bruckl T, Wagner M, Welzmler V, Michalakakis S, Muller M, Biel M, Carell T. Quantification of the sixth DNA base hydroxymethylcytosine in the brain. *Angew Chem Int Ed Engl* 2010;49:5375–7.
- Jin SG, Wu X, Li AX, Pfeifer GP. Genomic mapping of 5-hydroxymethylcytosine in the human brain. *Nucleic Acids Res* 2011;39:5015–24.
- Jin SG, Jiang Y, Qiu R, Rauch TA, Wang Y, Schackert G, Krex D, Lu Q, Pfeifer GP. 5-Hydroxymethylcytosine is strongly depleted in human cancers but its levels do not correlate with IDH1 mutations. *Cancer Res* 2011;71:7360–5.
- Figueroa ME, Abdel-Wahab O, Lu C, Ward PS, Patel J, Shih A, Li Y, Bhagwat N, Vasanthakumari A, Fernandez HF, Tallman MS, Sun Z, et al. Leukemic IDH1 and IDH2 mutations result in a hypermethylation phenotype, disrupt TET2 function, and impair hematopoietic differentiation. *Cancer Cell* 2010;18:553–67.
- Xu W, Yang H, Liu Y, Yang Y, Wang P, Kim SH, Ito S, Yang C, Xiao MT, Liu LX, Jiang WQ, Liu J, et al. Oncometabolite 2-hydroxyglutarate is a competitive inhibitor of alpha-ketoglutarate-dependent dioxygenases. *Cancer Cell* 2011;19:17–30.
- Kim YH, Pierscianek D, Mittelbronn M, Vital A, Mariani L, Hasselblatt M, Ohgaki H. TET2 promoter methylation in low-grade diffuse gliomas lacking IDH1/2 mutations. *J Clin Pathol* 2011;64:850–2.